RESPONSE BEHAVIOR OF LARGE-SCALE UNDERGROUND TANK DURING EARTHQUAKE

T. Shirasuna (I)
Y. Goto (II)
Presenting Author: T. Shirasuna

SUMMARY

This paper discusses the response behavior of a large-scale underground tank during earthquake showing earthquake observation data obtained on an existing underground tank. Deformations of the tank side wall due to earthquake are in two modes, oval and ring-shift patterns. To focus on the maximum value of tangential strains along the side wall, that of the ring-shift partern is twice the maximum value of the oval pattern in magnitude. Numerical simulations analyze the observed data and prove that ring-shift deformation is caused by incidence of shear waves from vertically below, while oval deformation is from planar variations in response of the surrounding ground.

INTRODUCTION

In Japan, in recent years, there have been projects to construct large numbers of cylindrical underground tanks of radii and depths as much as several tens of meters in order to store liquefied natural gas. The bodies of these underground tanks are of reinforced concrete construction and require advanced design techniques in arriving at their structural forms. Especially, the capacity to resist earthquake is of great concern since these tanks are usually built in newly reclaimed soft ground which is easily excited during earthquake. Moreover, as an underground tank is a flexible structure as a whole because of its very size, interactions between soil and tank during earthquake therefore greatly influence safety. This should be thoroughly considered in design.

With regard to earthquake responses of underground tanks, studies have been made by theoretical analyses, model experiments and earthquake observations. Some papers emphasize the response due to incidence of shear waves from vertically below (Ref. 1), while others emphasize the effect of surface waves travelling horizontally in the ground (Ref. 2). Earthquake-resistant designs of underground tanks in Japan have been made until today to cover both of these results on the conservative side. However, it is necessary for the behaviors of those tanks during earthquakes to be understood well in order to proceed with rational and economical earthquake-resistant design.

Consequently, the authors made observations of an actual large-sized underground tank with regard to its behaviors during earthquakes, and also analyzed the observed results through numerical simulations.

(I) Research Engineer, Technical Research Institute, OHBAYASHI-GUMI, Ltd., Tokyo, Japan
(II) Chief Research Engineer, Technical Research Institute, OHBAYASHI-GUMI, Ltd., Tokyo, Japan

UNDERGROUND TANK AND OBSERVATION DETAILS

The underground tank on which earthquake observation are being made is an embedded type semi-underground crude oil tank located at a water front industrial zone in the city of Yokohama in Kanagawa Prefecture (Fig. 1). The object of observations is a cylindrically shaped reinforced concrete retaining wall with a diameter of 68.6 m. This cylindrical wall is not in contact with tank proper, but possesses the same functions as the side wall of an ordinary underground tank. The ground structure is shown in Fig. 2. There is a layer of very soft fill at the top of the ground, while from a depth of 19 m is a mudstone layer. The underground tank has been constructed to penetrate into this mudstone layer.

The tank configuration and arrangement of instruments are shown in Fig. 3. The dynamic strains produced in the cylindrical wall and accelerations at the surrounding ground are being observed. Strains of the wall are being measured at both outer and inner sides of the wall at five locations 45 deg. apart on the circumference at the upper part of the wall. Two more points measuring strains in the vertical direction are located on the inner side of the wall. High-sensitivity strain meters of resolution power 0.01×10^{-6} are being used. In the surrounding ground, meanwhile, measuring points are at four locations, three at the ground surface, and one in the mudstone layer at the same depth as the bottom of the tank, where two-way component accelerometers are located. Observations were started on June 1979 and in the approximately 4 years since there have been more than ten earthqakes of JMA Intensity II (Modified Mercalli Intensity III) or higher. Of these earthquakes, the greatest one, JMA Intensiry IV, was Izu Hanto Toh-Oki Earthquake which occured on June 29, 1980. This earthquake was of magnitude 6.7, focal depth 10 km, and epicentral distance approximately 75 km. The study described hereafter in this paper is based on this earthquake record.

OBSERVATION RESULTS AND CONSIDERATIONS

Response of Ground Surrounding Tank

Acceleration records are shown in Fig. 4b. As shown in Table 1, a maximum acceleration at the ground surface of 97 gal was recorded. In the acceleration wave form of Fig. 4b, accelerations in the Y-direction are conspicuous for the principal motion at around 2 to 6 sec.

Fig. 5 shows the Fourier spectra of underground and ground surface acceleration records. The spectrum for the underground record is dispersed in a range up to 5 Hz, and conspicuous predominance of frequencies can not be seen. On the other hand, 2.7 Hz is markedly predominant in the spectrum for the ground surface and this is thought to be the appearance of the amplification property of the surface layer ground.

Response of Underground Tank

The earthquake records of strains produced in the underground wall of cylindrical shape are shown in Fig. 4a. Bending strains and axial strains were obtained from strain records of the outer and inner sides of the wall in accordance with the insert drawings of Fig. 6. The composite waveforms are given in Figs. 4c and 4d and the maximum values in Table 2. The Fourier spectra of typical waves are shown in Fig. 6.

In comparing bending and axial strains, it is seen that axial strain has

a larger value at the principal mortion part of the earthquake, following which bending develops. The predominant frequencies in the Fourier spectra of Fig. 6 show that the axial strain is well related to the motion of the ground surface, whereas the bending strain spectra has no conspicuous tendency.

Deformation Patterns of Underground

As a preparation for next section, the deformation patterns of the cylindrical underground wall are discussed using the pictures shown schematically in Fig. 7. The three patterns of ring-mode deformation A, in which shifting occurs while roughly maintaining a circular shape, and oval-mode deformation B and C with compression into egg shapes, are considered. Regarding the state of loading, it is thought a push and pull type of earthquake motion is acting for the ring-mode deformation of A. This corresponds to a case of uniform response of the ground surface due to incidence of shear wave from vertically below. Oval-mode deformations may be considered to be related to the strain conditions of the ground along the surface. It is thought that the compression type C is due to compressive deformation of the ground or deformation of the ground accompanying propagation of Rayleigh waves. The shear type B is due to in-plane strains of the ground or deformation of the ground accomanying propagation of Love waves.

Observed Deformation Patterns

The strain distribution diagram for any time can be prepared using Figs. 4c and 4d, and is shown in Fig. 8. The times t from a to h selected in Fig. 8 are entered in Fig. 4. In Fig. 8, the feature is that axial strains are large from a to d, and it is estimated that the cylindrical wall shows a ring-mode deformation pattern. The figures a and b were drawn to correspond to the times at which underground accelerations at the mudstone layer in which the wall is embedded indicate first-wave peaks. The wall sustains seismic load in the reverse direction of bedrock acceleration due to inertial force of the ground. The arrows in the figures indicate the directions of action. Figs. c and d are for times when axial strains of the wall indicate maximum values, and at these times accelerations at the ground surface also are close to maximum values.

Meanwhile, Figs. 8e to 8h were prepared focusing on oval modes seen in strain distributions in the circumferential direction. The broken lines at the upper halves are estimated lines imagining oval modes. Figs. 8e and 8g are estimated to indicate deformation patterns of shear-type oval modes. At these times, the ground showed shear deformations along its surface as indicated in the figures. Figs. 8f and 8h are estimated to show compression-type deformation patterns. The ground at such tiems is in states of compressive deformation, and it may be seen that there is good correspondence with deformation of the wall. However, the durations of time that the bending strain distributions of the wall during earthquake maintain the simple oval patterns picked up in Figs. 8e to 8h are short.

NUMERICAL ANALYSIS

Extraction of Ring-mode and Oval-mode Responses

In order to extract time domain responses, the tangential strain components of the cylindrical wall were assumed to be the following expansions:

$$Sa = \alpha s_1 \cdot \text{Sin}\ \theta + \alpha c_1 \cdot \text{Cos}\ \theta + \alpha s_2 \cdot \text{Sin}\ 2\theta + \alpha c_2 \cdot \text{Cos}\ 2\theta \quad \ldots\ldots\ (1)$$

$$Sb = \beta s_1 \cdot \text{Sin}\ \theta + \beta c_1 \cdot \text{Cos}\ \theta + \beta s_2 \cdot \text{Sin}\ 2\theta + \beta c_2 \cdot \text{Cos}\ 2\theta \quad \ldots\ldots\ (2)$$

where,
- Sa : axial strain as a function of t and
- sb : bending strain as a function of t and
- θ : angle at circumference of cylindrical coordinates
- $\alpha s_1 \sim \beta s_2$: Fourier series coefficients concerning axial or bending strains as a function of t

In the above equations, 0-order and 3rd-order-and-higher series were thought to have little influence and were omitted.

Then, using the ten observed strain records, the least squares method was applied to determine the eight coefficients α_{s1}-β_{c2} at every time step through the entire durations of the records. Figure 9 shows the time vairations of coefficients extracted in this way. As mentioned in the preceding chapter, the one-θ components of axial strains, α_{s1} and α_{c1} indicate time domain responses of ring mode, while the two-θ components of bending strains, β_{s2} and β_{c2}, correspond to responses of oval mode. Hence, Fig. 9 proves that the strains due to the ring mode are approximately twice those of oval-mode in magnitude.

Numerical Simulation on the Ring-mode Response

A finite element method on an axisymmetric structure with antisymmetric dynamic loading was used to calculate the one-θ response of the cylindrical wall. Figure 11 shows the model for the calculation. Material constants of the model were assumed based on in-situ measurements. An energy-transmitting boundary and free field elements were applied to the side boundary while the base boundary was taken to be fixed in consideration of the stiffness of mudstone. The earthquake waves recorded in the mudstone layer were the input waves at the rigid base.

Firstly, free field responses were calculated and compared with the ovserved records of the ground surface. A slight change in the assumed values of ground stiffness was needed to cause the predominant frequencies to coincide.

Next, the one-θ components of axial strains were obtained from the tank- and ground coupled-system calculation. The results are shown in Fig. 9 by dotted lines and compared. It is remarked that the calculated one-θ components are in good agreement with the extracted components except for the amplitude of the Sin θ case.

Numerical Simulation on Oval-mode Response

As it was necessary for the simulation to extract a two-θ component from the ground motion, Sin 2θ and Cos 2θ-components of the motion were assumed to be defined by the following equations:

$$Sgc = \frac{1}{3}(DX1 - DX3 - DY2 + \frac{1}{2}(DY1 + DY3)) \cdot \frac{\pi}{2R} \quad \ldots\ldots\ (3)$$

$$Sgs = \frac{1}{3}(DY1 - DY3 + DX2 - \frac{1}{2}(DX1 + DX3)) \cdot \frac{\pi}{2R} \quad \ldots\ldots\ (4)$$

where, Sgs, Sgc : strain amplitudes of Sin 2θ and Cos 2θ-components defined in Fig. 11 as functions of t
DY1 ∿ DX3 : displacements obtained from double intergral calculus of acceleration waves recorded at ground surfaces

Sgs and Sgc are shown in Fig. 12. The ratios of these ground strain levels to bending strain levels observed on the cylindrical wall that are β_{S2} and β_{C2} in Fig. 9, were approximately read from these figures as follows:

$$\beta_{S2} / Sgs = 0.065, \quad \beta_{C2} / Sgc = 0.055 \quad \ldots\ldots\ldots \quad (5)$$

On the other hand, the bending strain occurring in the ring which is surrounded by strained ground can be analytically estimated using the concept of the seismic deformation method, the details of which, however, are omitted here because of limits of space. In short, following the formula presented by Hamada (Ref. 2), the ratio of the strains was analytically estimated as follows:

$$\beta_S / Sg = 0.049 \quad \ldots\ldots\ldots\ldots\ldots \quad (6)$$

This analytical value is somewhat smaller than the values mentioned above. Moreover, the wave forms in Fig. 12 do not resemble well the forms of β_{S2} and β_{C2} in Fig. 9. In the last analysis, the distances between the measuring points of ground are thought to be too long to estimate the ground strains caused by horizontally travelling ripples, and analysis based on a concept of surface wave propagation may be necessary for a further study.

CONCLUSIONS

As a result of this study, a concept to serve as a basis in carrying out earthquake-resistant design of large underground tanks has been presented. However, the earthquake observations in the study were made at only a single location. As the response characteristic of an underground tank is apt to change according the surrounding ground condition and its structural configuration, further studies upon a number of other underground tanks are desired to be made.

ACKNOWLEDGEMENTS

The authors wish to express their heartfelt gratitude to Professor Keizaburo Kubo of the Faculty of Engineering, Saitama University, for much valuable advice in carrying out the study.

This study was conducted as a part of the technology development program of OHBAYASHI-GUMI, Ltd., and untiring assistance was received from Dr. Jiro Saito, Deputy Director of the Technical Research Institute of the company, to whom the authors owe their sincere thanks.

REFERENCES

1. Goto, Y. and Shirasuna, T., "Studies on Earthquake-Resistant Design of Grouped Underground Tanks in Soft Ground," Proceedings of the 8WCEE, 1984

2. Hamada, H., "Observations and Analysis for Seismic Behavior of a Large-scale Underground Tank," Proceedings of JSCE, No. 273, 1978. (in Japanese)

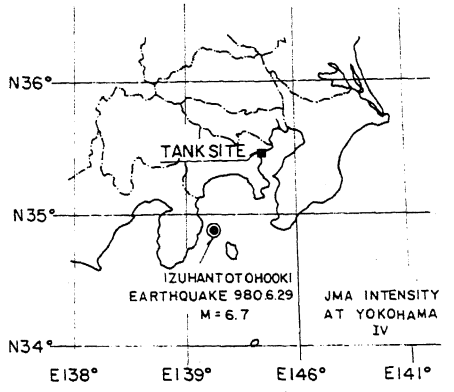

Fig. 1 Location of Epicenter and Tank

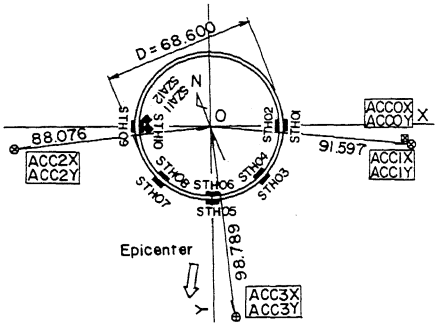

Fig. 2 Plan of Retaining Wall and Arrangement of Instruments (in mm)

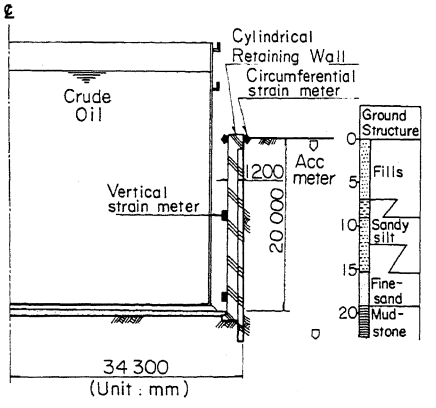

Fig. 3 Section of Wall and Ground Structure (in mm)

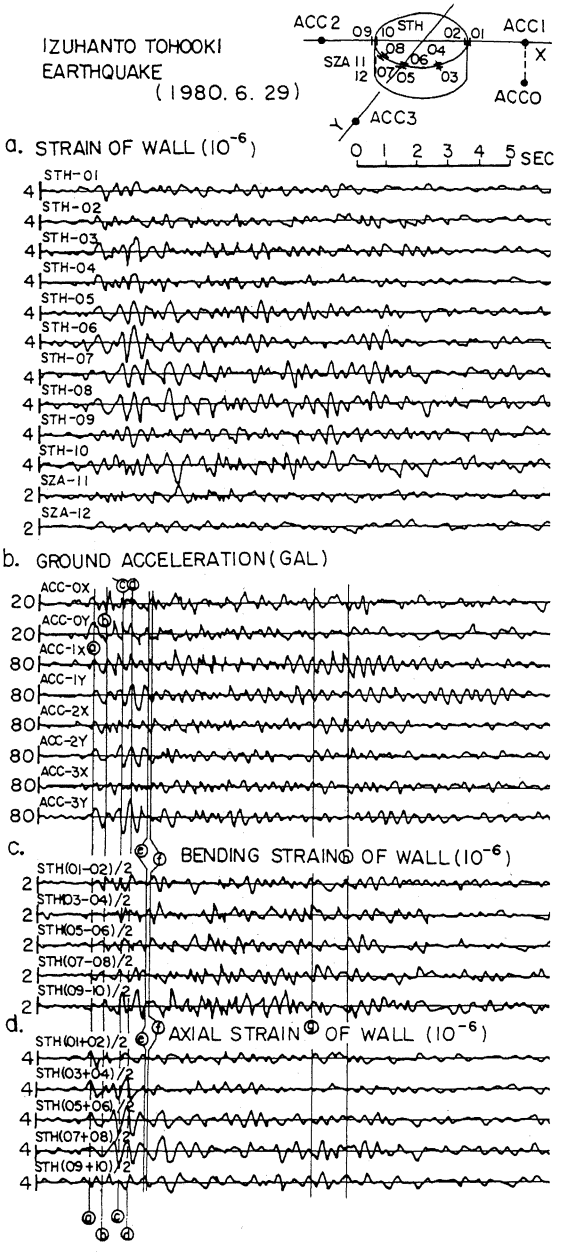

Fig. 4 Observed Records and Composite Waves

Table 1 Ground Accelerations

GROUND	POINT	MAX(GAL)	TIME(SEC)
BASE ACC.	ACC-0X	16.2	2.38
	ACC-0Y	15.2	3.40
SURFACE ACC.	ACC-1X	83.0	10.26
	ACC-1Y	97.7	3.32
	ACC-2X	48.1	3.76
	ACC-2Y	68.6	3.34
	ACC-3X	45.7	2.56
	ACC-3Y	92.9	3.06

Table 2 Bending and Axial Strains of Wall

WALL.ST.	PROCESS	MAX(10^{-6})	TIME(SEC)
BENDING STRAIN	STH(01-02)/2	1.38	7.13
	STH(03-04)/2	1.60	4.00
	STH(05-06)/2	1.64	5.69
	STH(07-08)/2	1.60	6.11
	STH(09-10)/2	2.34	4.50
AXIAL STRAIN	STH(01+02)/2	2.64	2.10
	STH(03+04)/2	3.12	2.84
	STH(05+06)/2	4.60	2.84
	STH(07+08)/2	4.48	2.85
	STH(09+10)/2	3.28	4.55

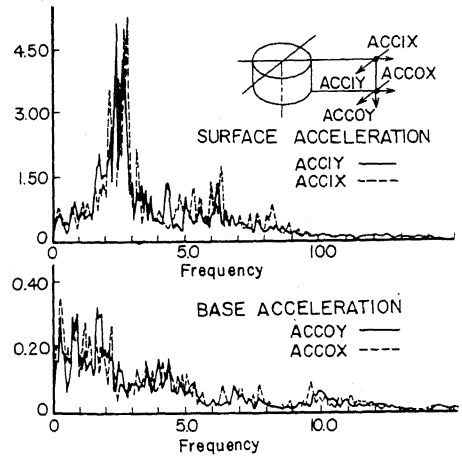

Fig. 5 Fourier Spectra of Underground and Ground Surface Acceleration Records

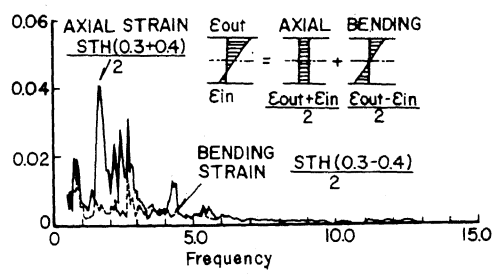

Fig. 6 Typical Fourier Spectrum of Wall Strain Records

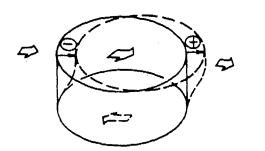

A. Push & pull type ring mode

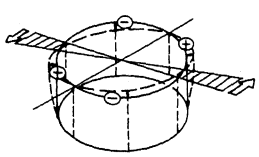

B. Shear type oval mode

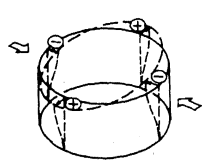

C. Compression type oval mode

Fig. 7 Idealized Deformations

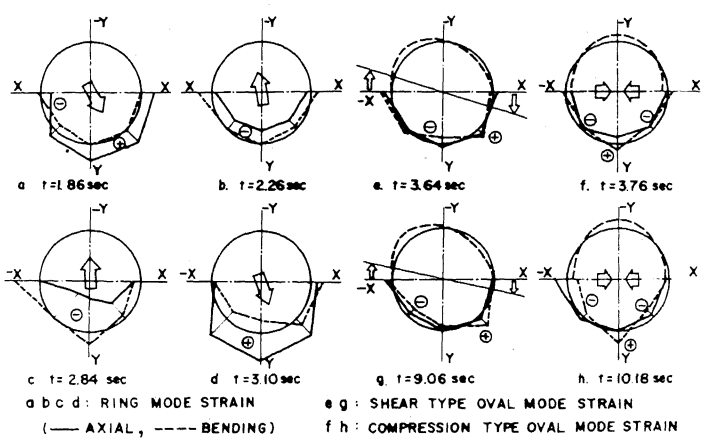

Fig. 8 Strain Distributions of Wall During Earthquake

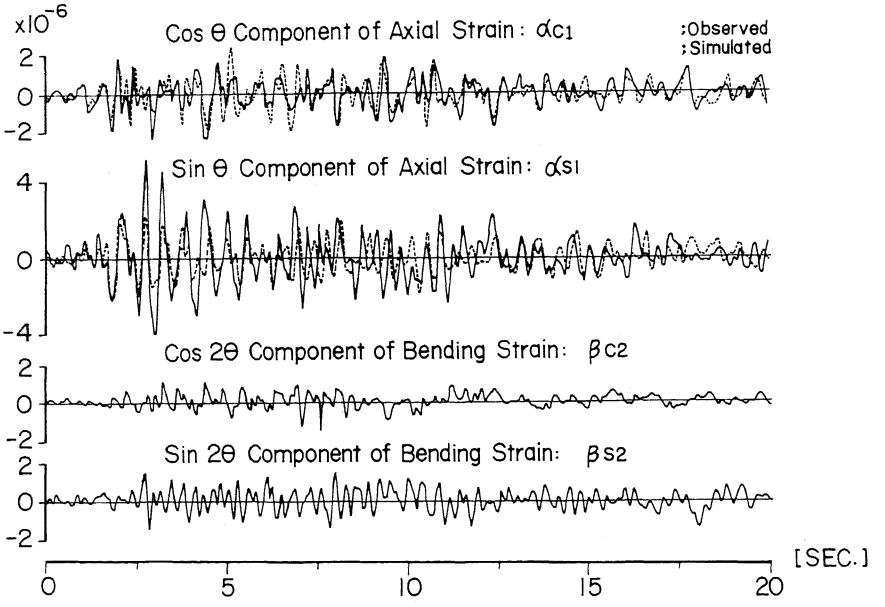

Fig. 9 Time Variations of Axial and Bending Strain Components

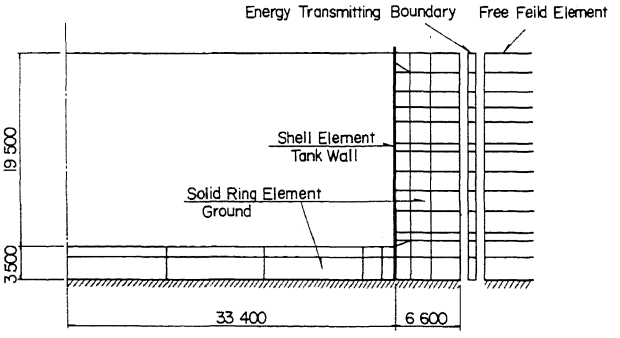

Fig. 10 Axisymmetric F.E.M. Model

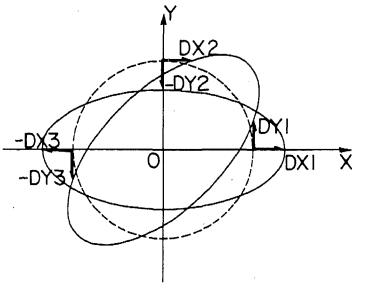

Fig. 11 Coordinate System for 2θ Components

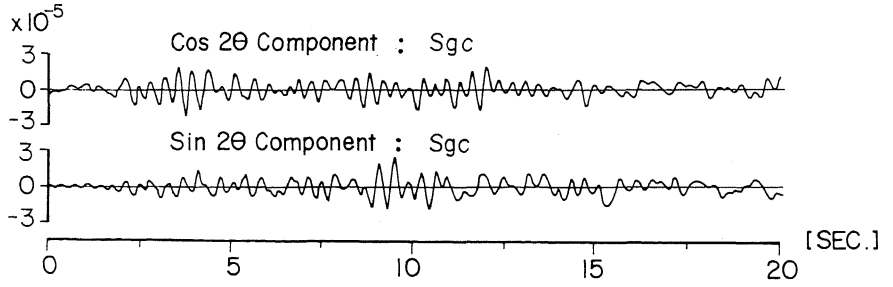

Fig. 12 Time Variations of Ground Strain 2θ Components